A R C H I V E S O F M E T A L L U R G Y A N D M A T E R I A L S
Volume 51 2006 Issue 3

J. WOJEWODA*, P. ZIĘBA*, R. ONDERKA*, R. FILIPEK**, P. ROMANÓW*

GROWTH KINETICS OF THE INTERMETALLICS FORMED IN DIFFUSION SOLDERED INTERCONNECTIONS

KINETYKA WZROSTU FAZ MIĘDZYMETALICZNYCH W SPOINIE UTWORZONEJ W WYNIKU LUTOWANIA DYFUZYJNEGO NISKOTEMPERATUROWEGO

The In-48 at.% Sn eutectic alloy was used in order to make Cu/Cu interconnection in the joining process called diffusion soldering. The sequence of intermetalic phases formation and their growth kinetics were determined by means of the light microscopy and scanning electron microscopy. This allowed to calculate the growth rate constant k and exponential factor n in the equation: $x = k \cdot t^n$ as well as to draw the diffusion path on the appropriate isotherm of Cu-In-Sn system. It was revealed that the η $[Cu_6(Sn,In)_5]$ phase appeared as the first one in the solid-liquid reaction between the Cu and In-Sn liquid and possessed dual morphology of fine and coarse grains. The deep grooves separating particular scallops of the η phase were considered to be "fast diffusion paths" at the early stage of the process. The gradual disappearance of grooves during further soldering makes the volume diffusion to be predominant way of mass transport.

The second intermetallic phase δ $[Cu_{41}(Sn,In)_{11}]$ was formed in the solid-solid reaction between the copper and η phase. It was observed either at lower temperatures after longer annealing time (tens of hours) or after short time (minutes) at 300°C and higher temperatures. This phase had rather regular interface and its growth was governed by the chemical reaction at the interface. The growth rate constant grew with the temperature and it was even three times higher then that one for the η phase. A short incubation time preceded the growth of this phase.

The fundamentals of mathematical model enabling the description of the growth of intermetallic phases in multi-component systems were presented.

Stop eutektyczny In-48 at.% Sn został zastosowany do utworzenia spoiny Cu/Cu w procesie lutowania dyfuzyjnego-niskotemperaturowego. Sekwencja tworzących się faz międzymetalicznych w spoinie oraz kinetyka ich wzrostu została opisana przy pomocy mikroskopii optycznej i skaningowej mikroskopii elektronowej. Pozwoliło to wyznaczyć stałą szybkości wzrostu oraz wykładnik potęgowy w równaniu: $x = k \cdot t^n$ oraz wykreślić tzw. ścieżkę dyfuzji w oparciu o przekroje izotermiczne układu Cu-Sn-In. Jako pierwsza tworzy się faza η $[Cu_6(Sn,In)_5]$ w reakcji między Cu i ciekłym stopem In-Sn. Posiada dwie morfologie różniące się wielkościami ziaren. Faza η w kontakcie z lutowiem tworzy charakterystyczne skalopki oddzielone od siebie wąskimi kanałami, które identyfikowane są jako ścieżki szybkiej dyfuzji w wczesnym stadium lutowania. Stopniowy zanik kanałów prowadzi do zwiększenia roli dyfuzji objętościowej jako czynnika kontrolującego kinetykę wzrostu faz w spoinie.

Druga faza międzymetaliczna δ $[Cu_{41}(Sn,In)_{11}]$ tworzy się podczas reakcji w stanie stałym między Cu i fazą η. Jej wzrost obserwowano w niższych temperaturach po kilkudziesięciu godzinach wygrzewania lub po kilku minutach lutowania w temperaturze 300°C i wyższych. Tworzenie się fazy δ poprzedzone jest krótkim okresem inkubacyjnym a jej wzrost kontrolowany jest reakcją na granicy faz. Stała szybkości wzrostu fazy δ wzrasta wraz ze wzrostem temperatury procesu i jest nawet trzy razy większa od stałej właściwej dla wzrostu fazy η. Przedstawiono podstawy modelu matematycznego dyfuzji w układach wieloskładnikowych, który może być wykorzystany do opisu wzrostu faz międzymetalicznych w spoinie.

1. Introduction

The expansion of microelectronics causes increased demands for interconnections – their reliability and resistance to the growing temperature and stress shocks. The goal is to find an appropriate composition of both technology and material to fulfil all the requirements. One of the problems encountered in the solder joints is unpredictable growth of the intermetallic phases (IPs). The irregular morphology of these phases, like long whiskers can be a reason of failures occurring during the service. The solution of these problems offers the diffusion-soldering technology. This process leads to the formation of the joint consisted solely of one or more

* INSTITUTE OF METALLURGY AND MATERIALS SCIENCE, POLISH ACADEMY OF SCIENCES, 3-059 KRAKÓW, 25 REYMONTA ST., POLAND
** FACULTY OF MATERIALS SCIENCE AND CERAMICS, AGH – UNIVERSITY OF SCIENCE AND TECHNOLOGY, 30-059 KRAKÓW, 30 MICKIEWICZA AV., POLAND

intermetallic phases, which can be easily predicted from the respective equilibrium phase diagram. The growth of such phase must be described in details to allow for designing soldering production line. The diffusion soldering process has already been studied by many authors [1–5]. In general, the process can be divided into four stages: heating, dissolution, isothermal solidification and the last one that governs the whole phenomenon – growth of the IPs. The IPs in the joint reveal high thermal stability, because the melting temperatures of the phases are higher than the applied solder. Several systems substrate/solder/substrate were investigated, among them detailed studies were performed on joining copper with either indium [6] or tin as interlayer [7] as well as nickel using tin [7] or aluminium interlayer [8]. All those studies reported on the binary component phases created in the interconnection area.

The present study concerns joining copper substrates using indium-tin eutectic alloy as a solder. This can lead to the formation of more complex intermetallic compounds. The In-48 at.%Sn solder could possibly stand for the banned conventional Pb-Sn solders in accordance with the European Directive. It reveals better wetability, higher ductility and longer fatigue life than the Pb-Sn alloy. Moreover, its relatively low melting temperature (118°C) allows joining substrates at the temperature slightly above it. The process is dedicated mainly to the electronic industry where the low temperature of production must be guaranteed. Therefore, gathering precise information about the growth kinetics of the intermetallics is crucial for designing and modelling all the phenomena occurring during manufacturing of the diffusion soldered joints.

2. Experimental procedure

Indium-tin eutectic alloy (48 at.% Sn) was prepared from the pure elements and melted in the high frequency furnace under protective atmosphere of argon. Then the alloy was cold-rolled to obtain a foil of 100 μm thick, which was subsequently kept in the furnace at 80°C for 1 month.

In order to obtain the diffusion soldered joints two copper (99.99% purity) slices were grinded on papers and cleaned in ultrasonic cleaner for 30 minutes. Then the In-48Sn foil was clamped between two Cu bars and hold at an appropriate temperature for different periods of time (Table 1).

The samples used for the microstructure observations, chemical analysis and kinetics determination were grinded using series of papers (600–2500), and then polished with the diamond paste (1–0.25 μm).

TABLE 1

Details of interconnection manufacturing

Temperature [°C]	Time of annealing [h]
180	1, 3, 4, 5
200	0.5, 1, 2, 3, 4, 5
220	0.5, 1, 2, 3, 4
250	0.25, 0.5, 1, 2, 4, 5
300	0.17, 0.33, 0.5, 0.83, 1
325	0.17, 0.33, 0.5, 0.83, 1
350	0.17, 0.33, 0.5, 0.83, 1

The observations of the microstructure were performed on a Scanning Electron Microscope (SEM) *Philips XL30* in secondary and backscattered electron regime with 20 kV accelerating voltage. Chemical analyses were carried out using an Energy Dispersive X-ray Spectrometer (EDX) Link *ISIS*. Quantitative analysis with ZAF correction method was performed with resulting relative error of 4%. The thickness measurements of IPs layer were accomplished with an optical microscope *Leica*. Because of the irregular character of the interface the mean value of about 100 measurements was taken to determine the thickness of each layer. The present study was performed with relatively large amount of the solder and the growing layer of intermetallic phase (IP) was several to dozen micrometers thick. This facilitated better accuracy of the measurements and the reduction of standard deviation. However, for application purposes the thickness of IPs has to be thinner to avoid brittle behaviour of the joint.

3. Results and discussion

3.1. Microstructure and chemical composition

The SEM observations revealed the formation of two IPs depending on the temperature of annealing. At temperatures below 250°C only one phase occurred. At higher temperatures (above 300°C) second IP was also present. The same behaviour was observed for longer time of annealing (more than 20 hours) at 200°C. In order to identify these phases, appropriate isothermal cross-sections of the ternary Cu-In-Sn phase diagram were calculated using PANDAT (ver. 5) software (Fig. 1). In the present work the self-consistent thermodynamic model assessed by the CALPHAD approach for Cu-In-Sn system by Liu et al. [9] was adopted. Binary interaction parameters were obtained from experimental data in previous works by least-squares minimization module PARROT (ThermoCalc Software) and collected in the COST 531 ver.2 (Lead free solder materials) database. For ternary system, a reliable thermodynam-

ic model was obtained using the information available from the binary systems plus any published ternary experimental data [9]. Liu et al. [9] described the Gibbs energies of the liquid, fcc and bcc phases by the subregular solution model and binary and ternary compounds are represented by the sublattice model.

The morphology of the first phase possessed dual character. A fine-grained thin layer was detected next to the copper substrate and a coarse-grained layer closer to the unreacted solder (Fig. 2a). The EDX microanalysis provided information that it was η phase. This phase is a high melting one and it is observed in the isothermal cross-section (Fig. 1) as the field between two sides of the G i b b s triangles Cu-In (Cu_2In) and Cu-Sn (Cu_6Sn_5). Two mechanisms of the η phase creation are possible:

1. Copper atoms diffuse through the η phase and react with the liquid at the solid/liquid interface and/or
2. Indium and tin atoms diffuse through the η phase and react at the Cu/η interface.

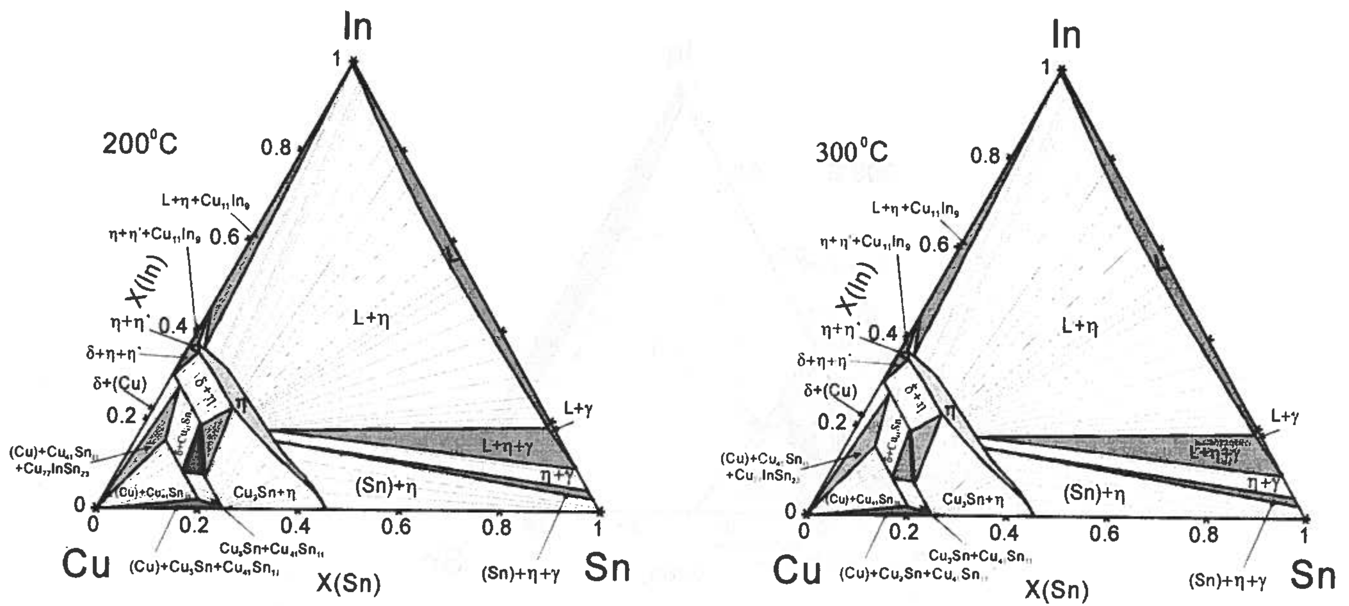

Fig. 1. Isothermal cross-sections of Cu-In-Sn phase diagram at 200°C (a) and 300°C (b) calculated from self-consistent thermodynamic model assessed by Liu et al. [9] using PANDAT software

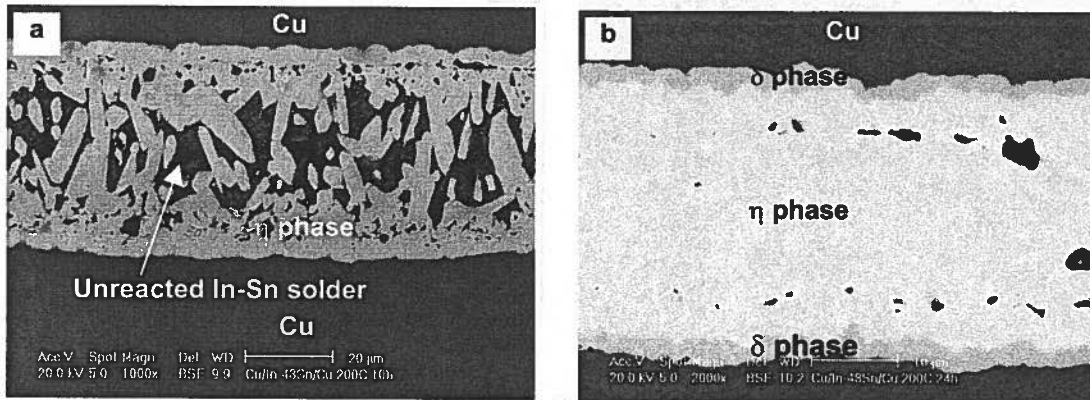

Fig. 2. SEM micrographs of diffusion-soldered interconnections: (a) dual morphology of η phase obtained at 200°C after 10 h of annealing. Unreacted solder is still visible in the central part of the joint, (b) η and δ phases in the interconnection area annealed for 24 hours at 200°C

Longer time of annealing even at 200°C resulted in the growth of second IP which is δ, based on the composition of $Cu_{41}(Sn,In)_{11}$. Its morphology was rather regular and it formed due to a solid state reaction between copper and η phase. At higher temperatures continous Cu diffusion to phase results in nucleation and precipitation of 5 phase at the CuIn interface.

A chemical analysis carried out across such a joint (Fig. 4) allowed for drawing the diffusion path in the isothermal cross-section of the ternary Cu-In-Sn diagram (Fig. 3). Two single phase fields were crossed by the diffusion path: η $[Cu_6(Sn,In)_5]$ and δ $[Cu_{41}(Sn,In)_{11}]$ which clearly confirmed the existence of these phases in the diffusion soldered area. The shape of the diffusion path in the L+η field: cutting the tie-lines indicated "wavy" character of the η phase interface. Moreover, the diffusion path gets closer into the indium corner direction. This suggests that the diffusion coefficient of tin in copper is higher than that of indium. The diffusion path cuts also δ $Cu_2(In,Sn)$ – ε $Cu_3(Sn,In)$ double phase field, however the ε phase was not observed. It can be explained by the fact that this phase is quickly consumed by the growth of δ phase or its amount was too small to be detected by the EDX analysis.

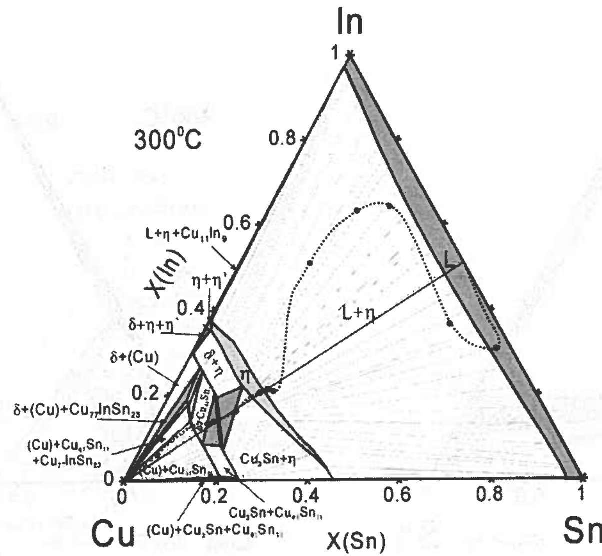

Fig. 3. Diffusion path for the Cu/In-Sn/Cu interconnection obtained at 300°C drawn on the isothermal cross-section of Cu-In-Sn

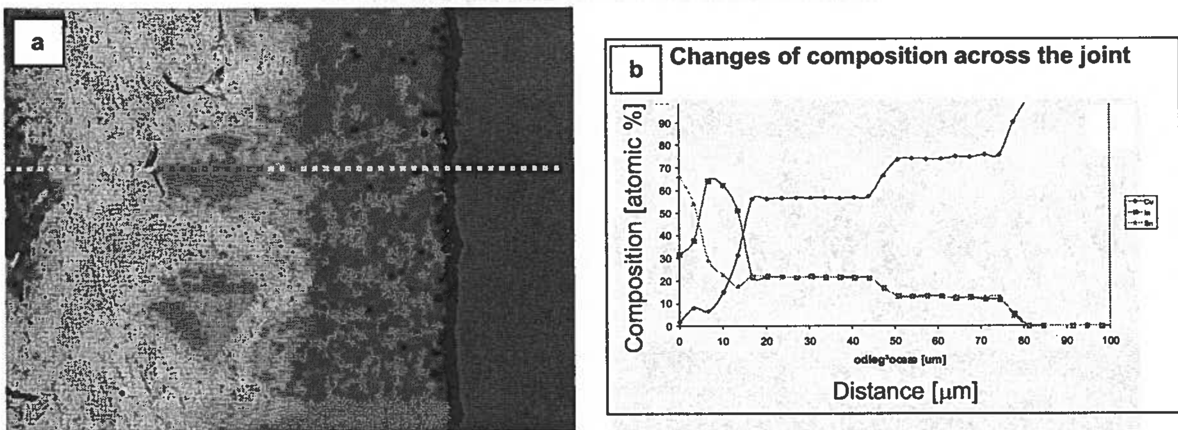

Fig. 4. Microstructure of Cu/In-48Sn/Cu joint obtained after 6 hours of annealing at 300°C (a) together with composition changes of Cu, In, Sn across the joint (b)

As the EDX analysis revealed chemical composition across the layer of IP to be constant (Fig. 4), therefore, determining diffusion coefficient using conventional M a t a n o - B o l t z m a n n analysis is no longer possible (when the concentration gradient approaches zero the diffusion coefficient approaches infinity). This problem will be considered in details in the Section 3.3.

3.2. The growth kinetics

Main information about the intermetallic growth kinetics is falling under the simple relation between the intermetallic phase thickness, x and time of annealing, t at appropriate temperature:

$$x = k \cdot t^n, \tag{1}$$

where k is the growth rate constant and n – the exponential factor.

The value of the exponent, n in the Eq. (1) equals to 0.5 indicates that the growth rate of the phase is controlled by volume diffusion. In this case Eq. (1) can be rewritten as:

$$x_p^2 = 2k_p t, \tag{2}$$

where the subscript p was introduced in order to emphasize the parabolic character of Eq. (2).

Also the choice of the proper formula: $x = f(t^{1/2})$ or $x^2 = f(t)$ must be carefully considered. P i e r a g g i [10] showed that $x = f(t^{1/2})$ matches in the situation when the IP formed in the beginning of the growth process (transition period of faster kinetics) does not influence the course of the next parabolic growth of this phase. In this case the following formula is valid:

$$x_p^2 = (x - x_i)^2 = 2k_p (t - t_i), \tag{3}$$

where x is the total thickness of the intermetallic layer after time t, x_i is the thickness of the layer after a preliminary period finished after time, t_i (after which the stabilized growth has begun), x_p is the width of the layer formed as a result of the parabolic growth started after time, t_i and corresponding to time $t - t_i$.

In this case the parabolic rate constants k_p resulting from the transformation of the Eq. (3) can be effectively calculated

$$x = x_i + \left(2k_p (t - t_i)\right)^{1/2}. \tag{4}$$

A second case may occur when the layer of thickness, x_i after a preliminary period has a significant influence on the stabilized parabolic growth period. Then the kinetic equation takes the following form:

$$x^2 - x_i^2 = 2k_p (t - t_i) \tag{5}$$

and the dependence $x^2 = f(t)$ allows to calculate the parabolic rate constant k_p. A similar situation occurs when stationary growth starts after an incubation period and there is no substantial transient period. In such a case $x_i = 0$ and the dependence $x^2 = f(t)$ gives the correct k_p values.

In our studies, the growth kinetics of both phases η and δ was investigated in the temperature range (180-250°C) and (300-350°C), respectively. Values of exponent factor, n together with the growth rate constant, k are collected in Table 2. They can be easily found when plotting $logx$ versus $logt$. The equation describing the straight line fitted to the data points:

$$\log x = n \log t + \log k \tag{6}$$

gave direct information about n and k.

TABLE 2

Values of exponential factor, n and growth rate constant, k for η and δ phasees at different temperatures

η phase	exponential factor n	growth rate constant k
180°C	0.26 ± 0.04	11.11 ± 0.47
200°C	0.29 ± 0.04	10.43 ± 0.49
220°C	0.31 ± (0.09)	11.27 ± 0.9
250°C	0.24 ± (0.02)	12.56 ± 0.27
δ phase	**exponential factor n**	**growth rate constant k**
300°C	1.12 ± 0.03	15.59 ± 0.45
325°C	1.10 ± 0.1	23.09 ± 2.27
350°C	0.93 ± 0.06	29.21 ± 1.63

When n equals to 0.5 the volume diffusion predominates as the growth controlling factor. Here, for the η phase, all the exponential factors were below 0.5 which means that volume diffusion together with other mechanism of diffusion occurred. As the η phase grew in the shape of hemispheres, deep grooves were present between them. They can work as paths for the fast diffusion in addition to the bulk diffusion through the η phase. Their further growth results in the gradual disappearance of these grooves.

The $x^2(t)$ dependence presented in Fig. 5 gave additional information about the growth of the h phase. The curve shape exhibits the important contribution of the fine grain structure in the beginning of the process, which brings about quicker growth of the phase during first few minutes. The curve attains characteristic shape for the volume diffusion growth after 2 hours of annealing. This corresponds to the dual microstructure observed with SEM (Fig. 2a).

As the η hemispheres grow with the temperature, the number of fast diffusion paths decreases which explains

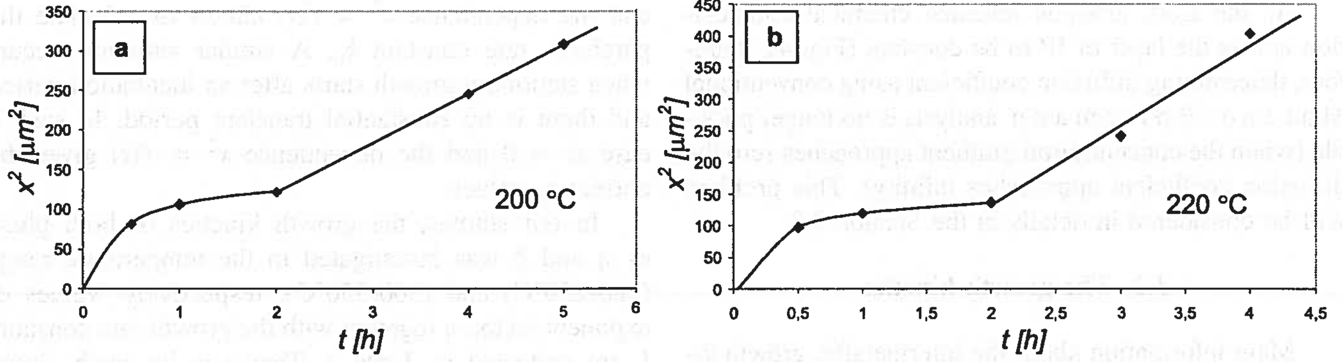

Fig. 5. Growth behaviour of η phase at 200°C (a) and 220°C (b)

the increasing value of n parameter. The n parameter becomes 0.24 at 250°C which is attributed to the presence of the thin layer of the δ phase. This phase was not detected during thickness measurements on the light microscopy. However, application of the higher magnification on the SEM clearly confirmed the presence of this phase.

A completely different behaviour was observed for the second intermetallic phase, δ. The process was governed by chemical reaction at the η/δ interface because the n factor was close to 1. The $logx(logt)$ dependence is plotted in Fig. 6 with the data points and straight line fitted to them in order to find n and k values. The growth stage of the δ phase is also preceded by the short incubation period.

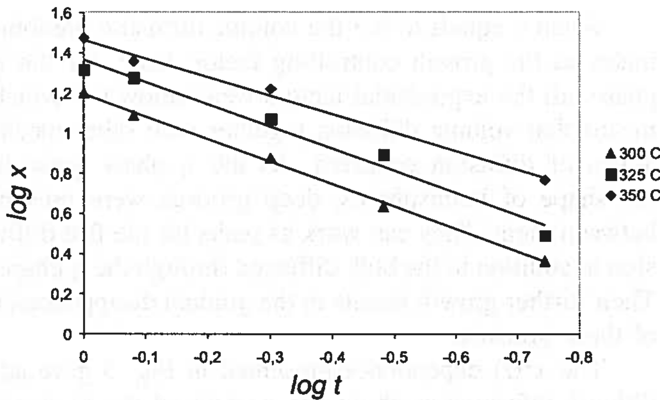

Fig. 6. Growth kinetics of the δ phase at 300°C, 325°C and 350°C

The growth of IP governed by chemical reaction (linear growth) shows important advantages. First of all, there is faster formation of the IP – here, within 2 hours the entire interconnection zone becomes occupied only by the δ phase, while in the case of η phase, the process required about 24 hours. Therefore, another advantage can be obtained – shorter time of production.

3.3. Mathematical model of the growth of intermediate phases in multi-component system

The diffusion soldering results in a number of intermediate phases, for which the ranges of composition have been observed to be very narrow. This makes serious difficulties when calculating the diffusion coefficient from the concentration profile because when the concentration gradient approaches zero then the diffusion coefficient approaches infinity.

Solution of the problem was given by Wagner [11], who derived the expression enabling to calculate chemical interdiffusion coefficient from the diffusion couple experiment. For any phase and composition N^* (assuming that the molar volume is constant, i.e., does not depend on the composition) the chemical interdiffusion coefficient can be calculated based on Sauer-Freise [12] and Boltzmann-Matano [13, 14] analysis

$$\tilde{D}(N^*) = \frac{1}{2t\,(\partial N/\partial x)_{x=x^*}}$$
$$\left[\frac{N^+ - N^*}{N^+ - N^-} \times \int_{-\infty}^{x^*} (N(x) - N^-)\,dx + \frac{N^* - N^-}{N^+ - N^-} \times \int_{x^*}^{\infty} (N^+ - N(x))\,dx\right], \quad (7)$$

where $N^* = N(x^*)$ means composition (in a mole fraction) for the position x^* for which $\tilde{D}(N^*)$ is calculated, $N^- = N(-\infty)$ and $N^+ = N(+\infty)$ are terminal compositions of the diffusion couple. The values of N in the brackets change from N^- to N^* for the first integral and from N^* to N^+ for the second one.

For intermediate phases having narrow homogeneity range one can assume linear concentration profiles, which allows integration of Eq. (7) and obtain the average interdiffusion coefficient for a phase, $\tilde{D}_{av}(N)$. Wagner [11] introduced a so-called integral diffusion coefficient, which is very useful for phases with very narrow homogeneity range

$$\tilde{D}^{i}_{\rm int} = \int_{N_1}^{N_2} \tilde{D} \mathrm{d}N = \tilde{D}_{\rm av}(N) \cdot \Delta N, \qquad (8)$$

where N_1 and N_2 are homogeneity limits of the considered phase, $\Delta N = N_2 - N_1$.

Equation (8) is valid for binary systems only and can not be used for multi-component ones. In this paper we consider the ternary system, Cu-In-Sn, and consequently different model, which takes into account ternary interactions, has to be applied. Such a model is being developed. Its new, original idea (apart from multi-component system) is the introduction of the flux constraint, which allows avoiding the non-physical, very high (if not infinite) fluxes at the very beginning of the process. The most important result of this concept is that it allows to estimate a delay of the formation of the slowly growing phases [15].

Modelling of the complex diffusion mass-transport process in multi-component systems requires: 1) kinetic data (mobilities/tracer diffusivities), 2) thermodynamic data (activities of the components) and 3) it has to include the drift velocity generated at the phase boundaries (interfaces). The intrinsic diffusion coefficients can be calculated as a product of thermodynamic factor and the mobilities/tracer diffusion coefficients of the elemental species in the phases of interest – Eq. (17). The thermodynamic factor is obtained from the phase equilibrium calculations using CALPHAD method [16, 17]. The mobilities/tracer diffusivities can be obtained e.g., from radiotracer diffusion measurements [18]. It is also possible to calculate mobilities from measured concentration profiles and solving a suitable inverse problem [19]. The model allows quantitative description of the growth of the flat intermediate layers under isothermal conditions formed by unlimited number of compounds. In the Figure 7, the formation of a single intermediate layer (β) between two primary phases (α and γ) is illustrated.

The evolution of concentration profiles of the elements in each phase is described by the law of mass conservation of an i-th component:

$$\frac{\partial c_i}{\partial t} = -\frac{\partial J_i}{\partial x} \quad (i = 1, ..., r). \qquad (9)$$

Following Darken drift flow idea we postulate that the flux of an i-th element is a sum of the diffusion flux, J_i^d, and drift flux:

$$J_i = J_i^d + c_i v. \qquad (10)$$

The effective solution of this model will be obtained using N e r n s t - P l a n c k diffusion flux formula [20]:

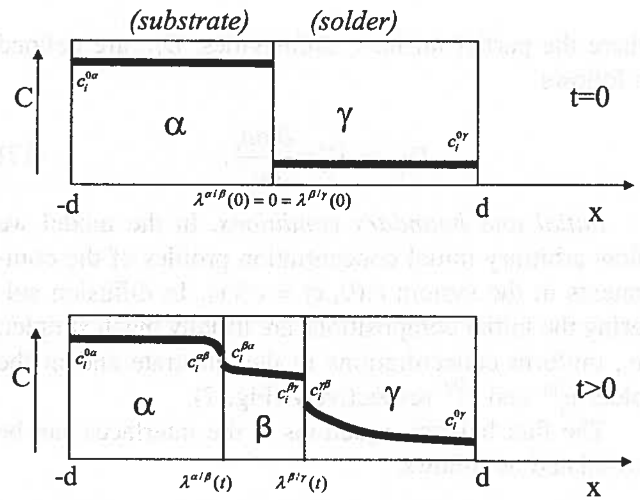

Fig. 7. Schematic presentation of growth of the intermediate phase β from the two primary phases α and γ

$$J_i^d = B_i c_i \sum_j F_j, \qquad (11)$$

where B_i is the mobility of an i-th component and $\sum_j F_j$ – the sum of the local driving forces. It is generally accepted, that in metallic systems (e.g. alloys) the diffusion force in Eq. (11) can be described as the spatial gradient of the chemical potential, μ_i, and the corresponding flux can be expressed by the following expression

$$J_i^d = -B_i c_i \frac{\partial \mu_i}{\partial x}. \qquad (12)$$

The chemical potential is expressed by

$$\mu_i (c_1, \ldots, c_r) = \mu_i^o + kT \ln a_i (c_1, \ldots, c_r), \qquad (13)$$

where k – the B o l t z m a n n ' s constant, T – an absolute temperature and μ_i^o is the standard-state chemical potential usually referred to unit thermodynamic activity ($a_i = 1$). The gradient of the chemical potential can be calculated as follows

$$\frac{\partial \mu_i}{\partial x} = \sum_{j=1}^{r} \frac{\partial \mu_i}{\partial c_j} \frac{\partial c_j}{\partial x}. \qquad (14)$$

Using Eqs. (12-14) and substituting the N e r n s t - E i n s t e i n relation $\left(D_i^* = B_i kT\right)$ the diffusion flux can be expressed as follows:

$$J_i^d = -D_i^* c_i \sum_{j=1}^{r} \frac{\partial \ln a_i}{\partial c_j} \frac{\partial c_j}{\partial x}. \qquad (15)$$

Above diffusion flux formula can be rearranged to a form used in calculations

$$J_i^d = -\sum_{j=1}^{r} D_{ij} \frac{\partial c_j}{\partial x}, \qquad (16)$$

where the partial intrinsic diffusivities, D_{ij}, are defined as follows

$$D_{ij} := D_i^* c_i \frac{\partial \ln a_i}{\partial c_j}. \tag{17}$$

Initial and boundary conditions. In the model we allow arbitrary initial concentration profiles of the components in the system $c_i(0,x) = c_i^o(x)$. In diffusion soldering the initial compositions are usually much simpler, i.e., uniform concentrations in the substrate and in the solder $c_i^{0\alpha}$ and $c_i^{0\gamma}$ respectively (Fig. 7).

The flux balance equations at the interfaces can be formulated as follows:

$$\begin{aligned} \left(c_i^{\alpha\beta} - c_i^{\beta\alpha}\right) \frac{d\lambda^{\alpha/\beta}}{dt} &= J_i^{\alpha\beta} - J_i^{\beta\alpha}, \\ \left(c_i^{\beta\gamma} - c_i^{\gamma\beta}\right) \frac{d\lambda^{\beta/\gamma}}{dt} &= J_i^{\beta\gamma} - J_i^{\gamma\beta} \quad i = 1, \ldots, r, \end{aligned} \tag{18}$$

where $\lambda^{\alpha/\beta}$, $\lambda^{\beta/\gamma}$ are positions of the α/β and β/γ interfaces and $d\lambda/dt$ – are their velocities; c_i^{jk} and J_i^{jk} – are the concentrations and fluxes of the i-th component in the j- phase at the interface j/k. In the case when a few intermediate phases are formed the boundary conditions (18) can be written for each interface.

If reactions at the interface are fast, compared to velocities of the phase interfaces, then local thermodynamic equilibrium can be assumed to hold at the interfaces. This hypothesis allows the boundary conditions to be determined – concentrations of the elements at the interfaces. Subsequently the diffusion problem given by Eqs. (9), (16) and (17) can be solved for each single-phase region. Finally, the velocities and positions of the interfaces are determined by solving the flux-balance Eqs. (18).

The intermediate phases formed during diffusion soldering can have very narrow ranges of homogeneity. In so-called-line compounds it is reasonable to assume average components' diffusivities and linear concentration profiles within such phase. These assumptions yield zero at second derivative of composition vs distance. Consequently, Eq. (9) can be ignored for the growth description of these intermediate phases and a time evolution of the boundary positions can be calculated much simpler, i.e., solving Eqs. (18) only.

Diffusion controlled delay of phase formation. It has been found that not all the intermediate phases present at the phase diagram are observed experimentally e.g., for Ni-Al system [21]. Here we postulate the constraints for fluxes. For every phase there exists maximum value of the diffusion flux:

$$J_i^d(\max) = D_i c_i / \lambda_i, \tag{19}$$

where λ_i denotes the characteristic distance for the diffusion (jump distance of defect). The phase exists if and only if the diffusion flux in this phase does not exceed $J_i^d(\max)$. Thus, this condition can be written as $J_i^d \leqslant J_i^d(\max)$.

Solution of the model. Equations describing growth of multi-component layers form system of nonlinear partial differential equations. Moreover, situation is even more complex because the position of interfaces changes with time, giving rise to the Stefan-like problems. Hence, we will look for a numerical solution using finite difference method. The details on the model and its numerical solution will be published [22].

4. Conclusions

The application of diffusion-soldering technology allowed for describing the growth kinetics of intermetallic phases which can form during joining of copper substrates with indium-tin foil. The η [$Cu_6(Sn,In)_5$] phase appeared as the first one in the solid-liquid reaction between the Cu and In-Sn liquid and possessed dual morphology of fine and coarse grains. The interface of η phase had "wavy" character which was also confirmed by the shape of the diffusion path. The deep grooves separating particular scallops entered the copper substrate. They were thought to be a "fast diffusion paths". Therefore, volume diffusion became the growth controlling factor after a certain time of reaction, while in the beginning the grain boundary diffusion played the important role.

With rising temperature the number of these grooves became smaller and this resulted in the increase of n parameter for the η phase. At 250°C the thin layer of new δ phase appeared which leads to the decrease of the n parameter to 0.24.

The second intermetallic phase: δ [$Cu_{41}(Sn,In)_{11}$] was formed in the solid-solid reaction between the copper and η phase. It was observed either at lower temperatures after longer annealing time (tens of hours) or after short time (minutes) at 300°C and higher temperatures. This phase had rather regular interface and its growth was governed by the chemical reaction at the interface. The growth rate constant grew with the temperature and it was even three times higher then that one for the η phase. A short incubation time preceded the growth of this phase.

The fundamentals of mathematical model enabling the description of the growth of intermetallic phases in multi-component systems were presented. The concept of flux constraint allows to estimate a delay of the formation of the slowly growing phases. In the present form

the model assumes that the process of growth of intermediate phases is controlled by diffusion of regents through the layers. Model is developed to allow both chemical reactions at the boundary and diffusion through the layers as the factors limiting the growth of phases. An important extension of the model is to consider non planar geometry of the interfaces. This involves description of the process in at least two dimension geometry as well as incorporation of the momentum equation to the model.

Acknowledgements

The Authors wish to express their gratitude to the Ministry of Science and High Education for the financial support under research project No. TO8C 02 829

REFERENCES

[1] G. Humpsten, D.M. Jacobson, Principles of soldering and brazing, ASM International, Materials Park, OH (1993).
[2] P.K. Khanna, S.K. Bhatnagar, L.S. Chang, W. Gust, Z. Metallkd. **90**, 470 (1999).
[3] W.F. Gale, J. Metals, February, **49** (1999).
[4] P.K. Khanna, S. Sommadossi, G. Lopez, E. Bielańska, P. Zięba, L.S. Chang, W. Gust, E.J. Mittemeijer, Conf. Proc., EUROMAT 99, edited by B. Jouffrey, J. Svejcar, Vol. 4, Willey-VCH, Weinheim, 219 (2000).
[5] P. Zięba, J. Wojewoda, Application of diffusion soldering in lead-free interconnection technology. In: Recent research developments in materials science 4, Research Signpost, Kerala, 261 (2003).
[6] S. Sommadossi, W. Gust, E.J. Mittemeijer, Mater. Sci. Techol. **19**, 528 (2003).
[7] S. Bader, W. Gust, H. Hieber, Acta Metall. Mater. **43**, 329 (1995).
[8] G. Lopez, P. Zięba, S. Sommadossi, W. Gust, E.J. Mittemeijer, Mater. Chem. Phys. **78**, 459 (2003).
[9] X.J. Liu, H.S. Liu, I. Ohnuma, R. Kainuma, K. Ishida, S. Itabashi, K. Kameda, K. Yamaguchi, J. Electr. Mater. **30**, 1093 (2001).
[10] B. Pieraggi, Oxid. Met. **27**, 177 (1987).
[11] C. Wagner, Acta Metall. **17**, 99 (1969).
[12] F. Sauer, V. Freise, Z. Elektrochem. **66**, 353 (1962).
[13] L. Boltzmann, Annal. Physik **53**, 960 (1884).
[14] C. Matano, Jap. J. Phys. **8**, 109 (1933).
[15] M. Danielewski, M. Wakihara, Defect and Diffusion Forum **237-240**, 151 (2005).
[16] L. Kaufman, B. Bernstein, "Computer Calculations of Phase Diagrams with Special Reference to Refractory Materials", Academic Press, New York (1970).
[17] U.R. Kattner, J. Phase Equlibria and Diffusion **27**, 126 (2006).
[18] S. Datta, R. Filipek, M. Danielewski, Defect and Diffusion Forum **203-205**, 47 (2002).
[19] S.V. Divinski, F. Hisker, Chr. Herzig, R. Filipek, M. Danielewski, Defect and Diffusion Forum **237-240**, 50 (2005).
[20] M. Planck, Ann. Phys. Chem. (Wiedemann) **39**, 161 (1890).
[21] L.S. Castleman, L.L. Siegle, Jour. Met. **9**, 1173 (1957).
[22] R. Filipek, P. Zięba, M. Danielewski, J. Wojewoda, K. Szyszkiewicz, "Mathematical model and numerical solution of the problem of the growth of intermediate phases", Computational Materials Science, in preparation.

Received: 10 May 2006.